Quality & Quantity
https://doi.org/10.1007/s11135-023-01813-6

Modeling the impact of control strategies on malaria and COVID-19 coinfection: insights and implications for integrated public health interventions

Adesoye Idowu Abioye[1] · Olumuyiwa James Peter[1,2] · Emmanuel Addai[3,4] · Festus Abiodun Oguntolu[5] · Tawakalt Abosede Ayoola[6]

Accepted: 22 November 2023

Abstract
This work discusses the challenge posed by the simultaneous occurrence of malaria and COVID-19 coinfection on global health systems. We propose a novel fractional order mathematical model malaria and COVID-19 coinfection. To assess the impact of control strategies on both diseases, we consider two control strategies which are, personal protection against mosquito bites ($u_1(t)$) and preventive measures for COVID-19 ($u_2(t)$). Numerical simulations demonstrate that consistent application of these measures leads to significant reductions in disease transmission. Using insecticide-treated nets and repellents during day and night effectively reduces malaria transmission, while implementing facial masks and hand hygiene controls COVID-19 spread. The most substantial impact is observed when both sets of protection measures are simultaneously adopted, highlighting the importance of integrated strategies. The study provides valuable insights into malaria and COVID-19 coinfection dynamics and emphasizes the impact of the control measures. of individual behavior and consistent adoption of personal protection measures to control both diseases. It underscores the need for integrated public health interventions to combat the dual burden of malaria and COVID-19, contributing to the development of targeted and efficient control measures.

Keywords Malaria · Covid-19 · Co-infection · Atangana–Baleanu derivative · Lyapunov function · Fractional order

✉ Olumuyiwa James Peter
peterjames4real@gmail.com

[1] Department of Mathematical and Computer Sciences, University of Medical Sciences, Ondo City, Nigeria

[2] Department of Epidemiology and Biostatistics, School of Public Health, University of Medical Sciences, Ondo City, Nigeria

[3] College of Biomedical Engineering, Taiyuan University of Technology, Shanxi 030024, Taiyuan, China

[4] Department of Mathematics, Taiyuan University of Technology, Shanxi 030024, Taiyuan, China

[5] Department of Mathematics, Federal University of Technology, Minna, Niger State, Nigeria

[6] Department of Mathematical Sciences, Osun State University, Osogbo, Osun State, Nigeria

Published online: 27 December 2023

1 Introduction

In the realm of global health, infectious diseases continue to pose significant challenges to public health systems. Two such diseases, malaria and COVID-19, have garnered worldwide attention due to their widespread prevalence and impact on human populations. Malaria, caused by Plasmodium parasites and transmitted through infected mosquito bites, has been a longstanding burden on several regions, primarily in sub-Saharan Africa, while COVID-19, caused by the novel coronavirus SARS-CoV-2, emerged as a global pandemic in 2019, affecting millions of people worldwide (Bwire et al. 2020). Although these diseases have distinct transmission routes and etiological agents, they share commonalities in their effects on human health and the potential for coinfection in susceptible individuals (Wesolowski et al. 2020; Wang et al. 2020).

Malaria and COVID-19 co-infection present an additional layer of complexity for healthcare systems, as it involves the simultaneous occurrence of both diseases in a single individual. Understanding the interplay between these two infections is crucial for implementing effective control strategies that address the challenges posed by their coexistence. Mathematical modelling has proven to be an invaluable tool in studying infectious diseases and evaluating the impact of various interventions on their spread and control. By developing a fractional order mathematical model that incorporates both malaria and COVID-19 dynamics, researchers can gain insights into the combined effects of control strategies, leading to more targeted and efficient public health measures (Chanda-Kapata et al. 2020).

Fractional order differential equations offer a more accurate representation of complex systems compared to traditional integer-order models. These equations allow for the inclusion of non-integer derivatives, capturing more intricate dynamics and offering a deeper understanding of the interactions between different disease components (Addai et al. 2023; Peter et al. 2022a, b, 2021; Zhu et al. 2022; Momani et al. 2020a, b; Maayah et al. 2022a, b). By utilizing a fractional order approach, researchers can analyze the intricate relationships between malaria and COVID-19 infections, considering various epidemiological parameters, immunity factors, and intervention measures.

The simultaneous occurrence of COVID-19 and malaria coinfection poses a significant challenge to global health systems, particularly in regions where both diseases are endemic. Mathematical modeling has emerged as a powerful tool for understanding the dynamics of infectious diseases and predicting the impact of various control strategies. In this literature review, we explore previous studies that have focused on developing mathematical models to investigate the coinfection dynamics of COVID-19 and malaria. By synthesizing the findings of these studies, we aim to identify key insights and potential areas for further research in the field of co-infections. To better understand the dynamics of co-infection of malaria and COVID-19 and other co-infection models, some studies have been developed (Tchoumi et al. 2021; Mekonen et al. 2022; Ojo et al. 2022; Avusuglo et al. 2022; Omame et al. 2021; Ojo and Goufo 2023). In this study, we build upon the model developed by Abioye et al. (2023) and enhance it by incorporating novel control strategies for both diseases. To the best of our knowledge, this work is unique as it considers the use of personal protection measures to prevent mosquito bites throughout the day and night. These measures include employing insecticide-treated nets, applying repellents to the skin, or using insecticide sprays. Additionally, we explore preventive practices such as physical distancing, maintaining good hand hygiene, and avoiding large gatherings. The incorporation of these control strategies is achieved through the application of a fractional optimal control approach. We aim to explore the impact of control strategies on the co-occurrence of malaria and COVID-19 using a novel fractional order mathematical model. Through this approach, we

hope to provide valuable insights into the efficacy of different public health interventions, such as vaccination campaigns, vector control, social distancing measures, and antimalarial drug distribution, on mitigating the burden of coinfection. Furthermore, the findings of this study can aid policymakers in devising integrated health strategies that address both diseases simultaneously, ensuring efficient allocation of resources and efforts to combat these health challenges. The remaining sections of the paper are organized as follows: Section two provides an overview of the study's preliminaries. In section three, the model formulation is discussed. The optimal control analysis is presented in section four, and section five covers the numerical simulations and discussion of results. Finally, in section six, the conclusions of the study are provided.

2 Preliminaries

In this section, let us recall some of the basic concepts such as definitions, theorems and other properties related fractional calculus that will be needed in our study.

Definition 1 (Atangana and Baleanu 2016) Let $\omega \in H^1(a,b)$, $a < b, \alpha \in [0,1]$, therefore, the Atangana–Baleanu–Caputo (ABC) fractional derivative of ω with order α is given by

$$ {}^{ABC}_{a}\mathcal{D}^{\alpha}_{t}[\omega(t)] = \frac{\mathfrak{A}(\alpha)}{1-\alpha}\int_a^t \dot{\omega}(\gamma)\mathbf{E}_{\alpha}\left[-\alpha\frac{(t-\gamma)^{\alpha}}{1-\alpha}\right]d\gamma \tag{1}$$

where $\mathfrak{A}(\alpha)$ is positive and is a normalization function fulfilling $\mathfrak{A}(0) = \mathfrak{A}(1) = 1$ and $\mathbf{E}_{\alpha}$ is the Mittag-Leffler function.

Definition 2 (Atangana and Baleanu 2016) Let $\omega \in H^1(a,b)$, $a < b, \alpha \in [0,1]$, therefore, the Atangana–Baleanu Riemann–Liouville (ABR) fractional derivative of ω with order α is given by

$$ {}^{ABR}_{a}\mathcal{D}^{\alpha}_{t}[\omega(t)] = \frac{\mathfrak{A}(\alpha)}{1-\alpha}\frac{d}{dt}\int_a^t \omega(\gamma)\mathbf{E}_{\alpha}\left[-\alpha\frac{(t-\gamma)^{\alpha}}{1-\alpha}\right]d\gamma \tag{2}$$

Definition 3 (Atangana and Baleanu 2016) Let $\omega \in H^1(a,b)$, $a < b, \alpha \in [0,1]$, therefore, the Atangana–Baleanu–Caputo (ABC) fractional Integral of a function $\omega(t)$ of order α is given by

$$ {}^{ABC}_{a}\mathcal{I}^{\alpha}_{t}[\omega(t)] = \frac{1-\alpha}{\mathfrak{A}(\alpha)}\omega(t) + \frac{\alpha}{\mathfrak{A}(\alpha)\Gamma(\alpha)}\int_a^t \omega(\sigma)(t-\sigma)^{\alpha-1}d\sigma \tag{3}$$

Definition 4 (Atangana and Baleanu 2016) The Laplace transform of Definitions 1 and 2 respectively can be written as

$$ \mathcal{L}\{{}^{ABC}_{0}\mathcal{D}^{\alpha}_{t}[\omega(t)]\}(p) = \frac{\mathfrak{A}(\alpha)}{1-\alpha}\frac{p^{\alpha}\mathcal{L}\{\omega(t)\}(p) - p^{\alpha-1}\omega(0)}{p^{\alpha} + \frac{\alpha}{1-\alpha}} \tag{4}$$

$$ \mathcal{L}\{{}^{ABR}_{0}\mathcal{D}^{\alpha}_{t}[\omega(t)]\}(p) = \frac{\mathfrak{A}(\alpha)}{1-\alpha}\frac{p^{\alpha}\mathcal{L}\{\omega(t)\}(p)}{p^{\alpha} + \frac{\alpha}{1-\alpha}} \tag{5}$$

where $\mathcal{L}$ is the Laplace transform operator.

Lemma 1 (Atangana and Baleanu 2016) *Let* $\omega \in H^1(a,b)$, $a < b, \alpha \in [0,1]$, *then the following inequality on* $[a,b]$ *is satisfied.*

$$ {}_{a}^{ABC}\mathcal{I}_t^{\alpha}\left({}_{a}^{ABC}\mathcal{D}_t^{\alpha}[\omega(t)]\right) = \omega(t) - \omega(a) \tag{6}$$

Theorem 2.1 (Atangana and Baleanu 2016) *The following inequality holds on a closed interval* $[a,b]$ *if* ω *be a continous function on* $[a,b]$

$$\|{}_{a}^{ABC}\mathcal{D}_t^{\alpha}[\omega(t)]\| < \frac{\mathfrak{L}(\alpha)}{1-\alpha}\|\omega(\gamma)\| \tag{7}$$

where

$$\|\omega(\gamma)\| = \max_{a\le t\le b}|\omega(\gamma)|$$

Theorem 2.2 (Atangana and Baleanu 2016) *The ABC and ABR fractional derivatives satisfy Lipschitz condition respectively as follows*:

$$\|{}_{0}^{ABC}\mathcal{D}_t^{\alpha}[\omega(t)] - {}_{0}^{ABC}\mathcal{D}_t^{\alpha}\left[g(t)\right]\| \le H\|\omega(t) - g(t)\| \tag{8}$$

$$\|{}_{0}^{ABR}\mathcal{D}_t^{\alpha}[\omega(t)] - {}_{0}^{ABR}\mathcal{D}_t^{\alpha}\left[g(t)\right]\| \le H\|\omega(t) - g(t)\| \tag{9}$$

Therefore, according to the Definition 3, the unique solution of the differential equation with fractional order α *can be written as*

$${}_{a}^{ABC}\mathcal{D}_t^{\alpha}[\omega(t)] = q(t)$$

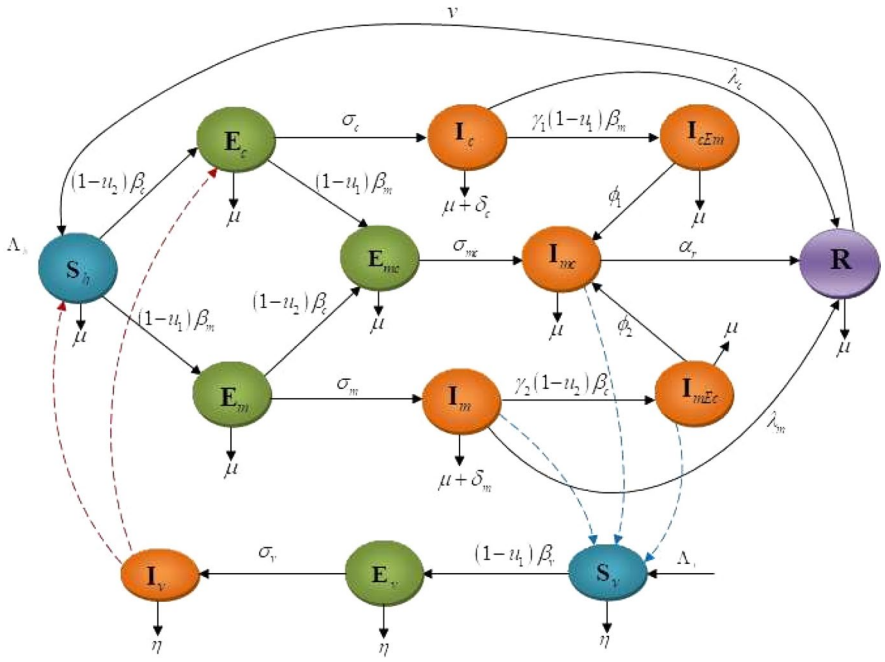

Fig. 1 Flow chart and the fractional Optimal control of Malaria-COVID-19 co-infection model

which means

$$\omega(t) = \frac{1-\alpha}{\mathfrak{L}(\alpha)} q(t) + \frac{\alpha}{\mathfrak{L}(\alpha)\Gamma(\alpha)} \int_a^t q(\sigma)(t-\sigma)^{\alpha-1} d\sigma \tag{10}$$

3 Model formulation

In this section, we extend the model proposed by Abioye et al. (2023) by introducing two control strategies, $u_1(t)$ and $u_2(t)$. $u_1(t)$ represents the use of personal protection measures to prevent mosquitoes bites during the day and the night such as the use of insecticide-treated nets, application of repellents to skin or spraying of insecticides at a time t, $u_2(t)$ represents practising physical distancing, maintaining good hand hygiene, and avoiding large gatherings. The specific formulation of the model is provided in the referenced study. As a result, the optimized control model for COVID-19, considering these two time-dependent control variables, is governed by a set of ordinary differential equations given in equation (11), and a visual representation of the model is depicted in Fig. 1.

$$\begin{aligned}
{}^{ABC}_{a}\mathcal{D}^{\alpha}_{t} S_h &= \Lambda_h - ((1-u_2)\beta_c + (1-u_1)\beta_m + \mu)S_h + \upsilon R_h \\
{}^{ABC}_{a}\mathcal{D}^{\alpha}_{t} E_c &= (1-u_2)\beta_c S_h - ((1-u_1)\beta_m + \sigma_c + \mu)E_c \\
{}^{ABC}_{a}\mathcal{D}^{\alpha}_{t} E_m &= \beta_m S_h - ((1-u_2)\beta_c + \sigma_m + \mu)E_m \\
{}^{ABC}_{a}\mathcal{D}^{\alpha}_{t} E_{mc} &= (1-u_1)\beta_m E_c + (1-u_2)\beta_c E_m - (\sigma_{mc} + \mu)E_{mc} \\
{}^{ABC}_{a}\mathcal{D}^{\alpha}_{t} I_c &= \sigma_c E_c - (\lambda_c + \gamma_1(1-u_1)\beta_m + \delta_c + \mu)I_c \\
{}^{ABC}_{a}\mathcal{D}^{\alpha}_{t} I_m &= \sigma_m E_m - (\lambda_m + \gamma_2(1-u_2)\beta_c + \delta_m + \mu)I_m \\
{}^{ABC}_{a}\mathcal{D}^{\alpha}_{t} I_{mc} &= \sigma_{mc} E_{mc} + \phi_1 I_{cEm} + \phi_2 I_{mEc} - (\alpha_r + \delta_{mc} + \mu)I_{mc} \\
{}^{ABC}_{a}\mathcal{D}^{\alpha}_{t} I_{cEm} &= \gamma_1(1-u_1)\beta_m I_c - (\phi_1 + \mu)I_{cEm} \\
{}^{ABC}_{a}\mathcal{D}^{\alpha}_{t} I_{mEc} &= \gamma_2(1-u_2)\beta_c I_m - (\phi_2 + \mu)I_{mEc} \\
{}^{ABC}_{a}\mathcal{D}^{\alpha}_{t} R_h &= \lambda_c I_c + \lambda_m I_m + \alpha_r I_{mc} - (\upsilon + \mu)R_h \\
{}^{ABC}_{a}\mathcal{D}^{\alpha}_{t} S_{\mathrm{v}} &= \Lambda_{\mathrm{v}} - (1-u_1)\beta_{\mathrm{v}} S_{\mathrm{v}} - \eta S_{\mathrm{v}} \\
{}^{ABC}_{a}\mathcal{D}^{\alpha}_{t} E_{\mathrm{v}} &= (1-u_1)\beta_{\mathrm{v}} S_{\mathrm{v}} - \sigma_{\mathrm{v}} E_{\mathrm{v}} - \eta E_{\mathrm{v}} \\
{}^{ABC}_{a}\mathcal{D}^{\alpha}_{t} I_{\mathrm{v}} &= \sigma_{\mathrm{v}} E_{\mathrm{v}} - \eta I_{\mathrm{v}}
\end{aligned} \tag{11}$$

where $\beta_c = \alpha_c(1-\epsilon\vartheta)(I_c + I_{mc} + I_{cEm})$;$\beta_{\mathrm{v}} = \alpha_{\mathrm{v}} b\left(I_m + I_{mc} + I_{mEc}\right)$; $\beta_m = \alpha_m b I_{\mathrm{v}}$;$\gamma_1, \gamma_2 \geq 0$ and where ${}^{ABC}_{a}\mathcal{D}^{\alpha}_{t}$ shows fractional derivative in ABC sense with initial conditions

$$\begin{aligned}
&S_h(0) = S_{h0}, E_c(0) = E_{c0}, E_m(0) = E_{m0}, E_{mc}(0) = E_{mc0}, \\
&I_c(0) = I_{c0}, I_m(0) = I_{m0}, I_{mc}(0) = I_{mc0}, I_{cEm}(0) = I_{cEm0}, \\
&I_{mEc}(0) = I_{mEc0}, R_h(0) = R_{h0}, S_{\mathrm{v}}(0) = S_{\mathrm{v}\,0}, \\
&E_{\mathrm{v}}(0) = E_{\mathrm{v}\,0}, I_{\mathrm{v}}(0) = I_{\mathrm{v}\,0}
\end{aligned} \tag{12}$$

The autonomous version of model (11) with the initial conditions (12) have been published in Tchoumi et al. (2021) and the following steps were carried out

i Existence and Uniqueness of Atangana–Baleanu–Caputo (ABC) with time fractional order COVID-19 and Malaria co-infection model solution.
ii Non-negativity of the solution for Malaria-only, COVID-19-only and their co-infection.
iii Existences of the Malaria-only-free, COVID-19-only-free and Malaria-COVID-19-free equilibria.
iv Basic reproduction numbers of malaria-only, COVID-19-only and their co-infection models.
v Existences of the endemic equilibria for malaria-only, COVID-19-only and their co-infection.
vi Global Stabilities of Malaria-only-free, COVID-19-only-free and Malaria-COVID-19-free equilibria.
vii Global Stabilities of endemic equilibria for Malaria-only and COVID-19-only and their co-infection.
viii Numerical solution of the fractional order of Malaria and COVID-19 model.

4 Fractional optimal control analysis (FOCA)

Optimal control has been a powerful tool used in Mathematical biology to minimise or reduce the number of infected malaria and COVID-19 humans in the population. Therefore, we propose a fractional order model of Malaria and COVID-19 co-infection to minimize the number of exposed humans to COVID-19, Malaria and Malaria-COVID-19. Also, to minimize infected humans to COVID-19, Malaria and Malaria-COVID-19 as well as minimizing total population of mosquitoes. We consider two control strategies and these are: $u_1(t)$ and $u_2(t)$

To achieve this from model (11), the following steps must be adhered: To

i describe of fractional optimal control.
ii show the existence of fractional optimal control.
iii show the uniqueness of fractional optimal control.
iv solve the fractional optimal control numerically.
v show the effects of control variables graphically on the model.

4.1 Description of fractional optimal control

The objective function of the fractional optimal control model developed in model (11) can be defined as

$$\mathcal{J} = \int_0^{t_f} \Big(X_1(I_m + I_{mEc}) + X_2(I_c + I_{cEm}) + X_3 I_{mc} + X_4 N_v + \frac{1}{2} Y_1 u_1^2(t) + \frac{1}{2} Y_2 u_2^2(t) \Big) dt, \tag{13}$$

where X_1, X_2, X_3, X_4, Y_1, and Y_2 be positive weight constants representing the infected human population with malaria, infected human population with COVID-19, co-infected human population with both malaria and COVID-19, total mosquito population, personal protection measures to prevent mosquito bites, and personal protection measures to prevent oneself against Coronavirus, respectively. Additionally, $Y_1 u_1^2(t)$ and $Y_2 u_2^2(t)$ are the quadratic costs associated with preventing mosquito-human (vector-host) contacts and coronavirus contacts, respectively.. We considered the objective function and quadratic cost according

to Peter et al. (2021); Tchoumi et al. (2021); Atangana and Baleanu (2016); Okuonghae and Omame (2020); Orwa et al. (2022); Abioye et al. (2018). Our purpose is to see the effect or impart of control strategies incorporated on the fractional model developed earlier in Peter et al. (2021) by finding control variables $u_1(t)$ and $u_2(t)$ by using the optimal control $u_1^*(t)$ and $u_2^*(t)$ such that

$$\mathcal{J}(u_1^*, u_2^*) = min\{(u_1, u_2) : u_1, u_2 \in \phi\} \tag{14}$$

where $\phi = \{u_i : 0 \leq u_i(t) \leq 1$, Lebesque measureable $t = [0, t_f]$ for $i = 1, 2\}$ is the control set.

4.2 Existence of fractional optimal control (EFOC)

The fractional optimal control model developed can only exist if all necessary conditions satisfying the Pontryagin's maximum principle (PMP) (Boltyanskiy et al. 1962). It is important that we consider Eqs. (13) and (14) in fractional order and applied PMP to convert Eqs. (11), (14) and (14) into a problem of minimizing point-wise Lagrangian. For convenience, we write "$S_h, E_m, E_c, E_{mc}, I_m, I_c, I_{mc}, I_{cEm}, I_{mEc}, R_h, S_{\mathrm{v}}, E_{\mathrm{v}}, I_{\mathrm{v}}$" as "$S_h, E_m, \ldots, I_{\mathrm{v}}$" and "$S_h^*, E_m^*, E_c^*, E_{mc}^*, I_m^*, I_c^*, I_{mc}^*, I_{cEm}^*, I_{mEc}^*, R_h^*, S_{\mathrm{v}}^*, E_{\mathrm{v}}^*, I_{\mathrm{v}}^*$" as "$S_h^*, E_m^*, \ldots, I_{\mathrm{v}}^*$". Therefore, we have

$$\mathcal{J}(u_1, u_2) = \int_0^{t_f} \eta\big(S_h, E_m, \ldots, I_{\mathrm{v}}, u_1, u_2, t\big)dt \tag{15}$$

subject to the constraints

$$\underset{a}{^{ABC}}\mathcal{D}_t^{\alpha}\psi_j = \xi_i \tag{16}$$

where

$$\xi_i = \xi_i\big(S_h, E_m, \ldots, I_{\mathrm{v}}, u_1, u_2, t\big)$$

and

$$\psi_j = \big(S_h, E_m, \ldots, I_{\mathrm{v}}, u_1, u_2, t\big)$$

for $i = 1, 2, 3, \ldots, 13$ and $j = 1, 2, 3, \ldots, 13$ respectively, and satisfying the conditions $\psi_1(0) = S_{h0}, \psi_2(0) = E_{m0}, \psi_3(0) = E_{c0}, \ldots, \psi_{13}(0) = I_{\mathrm{v}\,0}$.

According to Abioye et al. (2020) and Sweilam et al. (2020), we consider a modified cost functional

$$\tilde{\mathcal{J}} = \int_0^{t_f} \{H\big(S_h, E_m, \ldots, I_{\mathrm{v}}, u_1, u_2, t\big) + \sum_{i=1}^{13} \lambda i \xi_i\big(S_h, E_m, \ldots, I_{\mathrm{v}}, u_1, u_2, t\big)\}dt \tag{17}$$

Therefore, the Hamiltonian (H) can be defined as

$$\begin{aligned} H\big(S_h, E_m, \ldots, I_{\mathrm{v}}, u_1, u_2, \lambda i, t\big) =& \eta\big(S_h, E_m, \ldots, I_{\mathrm{v}}, u_1, u_2, \lambda i, t\big) \\ &+ \sum_{i=1}^{13} \lambda i \xi_i\big(S_h, E_m, \ldots, I_{\mathrm{v}}, u_1, u_2, \lambda i, t\big) \end{aligned} \tag{18}$$

Hence, the existence of fractional optimal control (11) can be stated using the theorem below (Abioye et al. 2020) and Sweilam et al. (2020),

Theorem 4.1 *An optimal control* $u_i^* \in \phi$ *for* $i = 1, 2$ *exists such that* $\mathcal{J}(u_1^*, u_2^*) = min\{(u_1, u_2) : u_1, u_2 \in \phi\}$ *subject to the fractional control model* (11) *with initial conditions at* $t = 0$.

Proof The state and control variables of the model (11) are non-negative values and control set ϕ is closed and convex. So the integrand of Eq. (13) that is, the objective function of the model which was stated in model (11) is a convex function of (u_1, u_2) on the control set ϕ. Therefore, if the state solutions are bound then the Lipschits property of that state model with respect to the state variables is satisfied. It is obvious that there exists non-negative numbers Υ_1, Υ_2 and a constant $\varrho > 1$ such that

$$\mathcal{J}(u_1, u_2) \geq \Upsilon_1 \left(|u_1|^2, |u_2|^2\right)^{\frac{\varrho}{2}} - \Upsilon_2 \tag{19}$$

□

Finally, the existence of the fractional optimal control (11) showed that the state variables are bounded.

4.3 Uniqueness of fractional optimal control (UFOC)

The necessary conditions for the factional optimal control can be satisfied if we consider Pontryagin's Maximum Principle. Based on this fact that the objective function in Eq. (13) derived from the model (11) which showed the existence of fractional control can be described as follows:

$${}_{t}^{ABC}\mathcal{D}_{tf}^{\alpha}(\lambda_j) = \frac{\partial H(t, \psi_j, u_i, \lambda_j)}{\partial \psi_j}, \qquad j = 1, 2, 3, \ldots, 13; \quad i = 1, 2 \tag{20}$$

where $\psi_j = \left(S_h, E_m, \ldots, I_{\mathrm{v}}, u_1, u_2, t\right)$,

$$0 = \frac{\partial H(t, \psi_j, u_i, \lambda_j)}{\partial u_i}, \qquad j = 1, 2, 3, \ldots, 13; \quad i = 1, 2 \tag{21}$$

and

$${}_{0}^{ABC}\mathcal{D}_{tf}^{\alpha}(\psi_j) = \frac{\partial H(t, \psi_j, u_i, \lambda_j)}{\partial \lambda_j}, \qquad j = 1, 2, 3, \ldots, 13; \quad i = 1, 2 \tag{22}$$

In view of this, it is important that Lagrange multipliers satisfies the transversality conditions

$$\lambda_j(t_f) = 0, \qquad j = 1, 2, 3, \ldots, 13 \tag{23}$$

From Eq. (20), we have,

$$ {}_{t}^{ABC}\mathcal{D}_{tf}^{\alpha}(\lambda_j) = \frac{\partial H(t, \psi_j, u_i, \lambda_j)}{\partial \psi_j}, \qquad j = 1, 2, 3, \ldots, 13; \quad i = 1, 2 $$

and Eq. (22), that is,

$$ {}_{0}^{ABC}\mathcal{D}_{tf}^{\alpha}(\psi_j) = \frac{\partial H(t, \psi_j, u_i, \lambda_j)}{\partial \lambda_j}, \qquad j = 1, 2, 3, \ldots, 13; \quad i = 1, 2 $$

we obtain

$$
\begin{aligned}
{}_{t}^{ABC}\mathcal{D}_{tf}^{\alpha}(\lambda_1) &= -\frac{\partial H}{\partial S_h} = (1-u_1)\beta_m(\lambda_1-\lambda_3) + (1-u_2)\beta_c(\lambda_1-\lambda_2) + \mu\lambda_1 \\
{}_{t}^{ABC}\mathcal{D}_{tf}^{\alpha}(\lambda_2) &= -\frac{\partial H}{\partial E_c} = (1-u_1)\beta_m(\lambda_2-\lambda_4) + \sigma_c(\lambda_2-\lambda_5) + \mu\lambda_2 \\
{}_{t}^{ABC}\mathcal{D}_{tf}^{\alpha}(\lambda_3) &= -\frac{\partial H}{\partial E_m} = (1-u_2)\beta_c(\lambda_3-\lambda_4) + \sigma_m(\lambda_3-\lambda_6) + \mu\lambda_3 \\
{}_{t}^{ABC}\mathcal{D}_{tf}^{\alpha}(\lambda_4) &= -\frac{\partial H}{\partial E_{mc}} = \sigma_{mc}(\lambda_4-\lambda_7) + \mu\lambda_4 \\
{}_{t}^{ABC}\mathcal{D}_{tf}^{\alpha}(\lambda_5) &= -\frac{\partial H}{\partial I_c} = \alpha_c(1-u_2)(1-\epsilon\vartheta)((\lambda_1 \\
&\quad -\lambda_2)S_h + (\lambda_3-\lambda_4)E_m) + \gamma_1\beta_m(1-u_1)(\lambda_5-\lambda_8) \\
&\quad +\lambda_c(\lambda_5-\lambda_{10}) + (\delta_c+\mu) \\
{}_{t}^{ABC}\mathcal{D}_{tf}^{\alpha}(\lambda_6) &= -\frac{\partial H}{\partial I_m} = \gamma_2\beta_c(1-u_2)(\lambda_6-\lambda_9) + \lambda_m(\lambda_6-\lambda_{10}) + (1-u_1)\alpha_{\mathrm{v}}\, b(\lambda_{11}-\lambda_{12}) \\
&\quad +(\delta_m+\mu)\lambda_6 - X_1 \\
{}_{t}^{ABC}\mathcal{D}_{tf}^{\alpha}(\lambda_7) &= -\frac{\partial H}{\partial I_{mc}} = \alpha_c(1-u_2)(1-\epsilon\vartheta) \\
&\quad ((\lambda_1-\lambda_2)S_h + (\lambda_3-\lambda_4)E_m) + \gamma_2(1-u_2)(\lambda_6-\lambda_9)I_m \\
&\quad +\alpha_{\mathrm{v}}\, b(1-u_1)(\lambda_{11}-\lambda_{12})S_{\mathrm{v}} + \alpha_r(\lambda_7-\lambda_{10}) + (\delta_{mc}+\mu)\lambda_7 - X_3 \\
{}_{t}^{ABC}\mathcal{D}_{tf}^{\alpha}(\lambda_8) &= -\frac{\partial H}{\partial I_{cEm}} = \alpha_c(1-u_2)(1-\epsilon\vartheta) \\
&\quad ((\lambda_1-\lambda_2)S_h + (\lambda_3-\lambda_4)E_m + \gamma_2(\lambda_6-\lambda_9)I_m) \\
&\quad +\phi_1(\lambda_8-\lambda_7) + \mu\lambda_8 - X_2 \\
{}_{t}^{ABC}\mathcal{D}_{tf}^{\alpha}(\lambda_9) &= -\frac{\partial H}{\partial I_{mEc}} = \phi_2(\lambda_9-\lambda_7) + \alpha_{\mathrm{v}}\, b(1-u_1)(\lambda_{11}-\lambda_{12}) + \mu \\
{}_{t}^{ABC}\mathcal{D}_{tf}^{\alpha}(\lambda_{10}) &= -\frac{\partial H}{\partial R_h} = \upsilon(\lambda_{10}-\lambda_1) + \mu\lambda_{10} \\
{}_{t}^{ABC}\mathcal{D}_{tf}^{\alpha}(\lambda_{11}) &= -\frac{\partial H}{\partial S_{\mathrm{v}}} = \beta_{\mathrm{v}}(1-u_1)(\lambda_{11}-\lambda_{12}) + \eta\lambda_{11} - X_4 \\
{}_{t}^{ABC}\mathcal{D}_{tf}^{\alpha}(\lambda_{12}) &= -\frac{\partial H}{\partial E_{\mathrm{v}}} = \sigma_{\mathrm{v}}(\lambda_{12}-\lambda_{13}) + \eta\lambda_{12} - X_4 \\
{}_{t}^{ABC}\mathcal{D}_{tf}^{\alpha}(\lambda_{13}) &= -\frac{\partial H}{\partial I_{\mathrm{v}}} = \alpha_m b(1-u_2)((\lambda_1-\lambda_3)S_h \\
&\quad +(\lambda_2-\lambda_4)E_c + (\lambda_5-\lambda_8)I_c) + \eta\lambda_{13} - X_4
\end{aligned}
\tag{24}
$$

Theorem 4.2 (Abioye et al. 2020) *and Sweilam et al.* (2020), *If we consider* $S_h^*, E_m^*, \ldots, I_{\mathrm{v}}^*$ *to be optimal state solutions as well as optimal control variables* u_1^* *and* u_2^* *for the fractional optimal control model* (11) *and its objective function in Eq.* (13), *then* $\exists$ *adjoint variables* $\lambda_j, \quad j = 1, 2, 3, \ldots, 13$ *which satisfy the adjoint Eq.* (24) *given in the Appendix, the transversality conditions*

$$\lambda_j(t_f) = 0, \qquad j = 1, 2, 3, \ldots, 13 \tag{25}$$

and the optimality conditions

$$H(S_h^*, E_m^*, \ldots, I_{\mathrm{v}}^*, u_1^*, u_2^*, \lambda_j) = \min_{0 \le u_1, u_2 \le 1} H(S_h^*, E_m^*, \ldots, I_{\mathrm{v}}^*, u_1^*, u_2^*, \lambda_j) \tag{26}$$

for $j = 1, 2, 3, \ldots, 13$. *Furthermore*,

$$\begin{aligned} u_1^* &= \max\left\{0, \min\left\{1, \frac{\mathfrak{B}_1}{Y_1}\right\}\right\} \\ u_2^* &= \max\left\{0, \min\left\{1, \frac{\mathfrak{B}_2}{Y_2}\right\}\right\} \end{aligned} \tag{27}$$

where $\mathfrak{B}_1 = \beta_m S_h(\lambda_3 - \lambda_1) + \beta_m E_c(\lambda_4 - \lambda_2) + \lambda_1 \beta_m I_c(\lambda_8 - \lambda_5) + \beta_{\mathrm{v}} S_{\mathrm{v}}(\lambda_{12} - \lambda_{11})$ *and* $\mathfrak{B}_2 = \beta_c S_h(\lambda_2 - \lambda_1) + \beta_c E_m(\lambda_4 - \lambda_3) + \lambda_2 \beta_c I_m(\lambda_8 - \lambda_6)$

Proof We obtain Eq. (24) from Eqs. (20) and (22). Therefore, Hamiltonian defined in Eq. (18) can now be written as

$$\begin{aligned} H^* =& X_1\left(I_m^* + I_{mEc}^*\right) + X_2\left(I_c^* + I_{cEm}^*\right) + X_3 I_{mc}^* + X_4 N_{\mathrm{v}}^* + \frac{1}{2} Y_1 u_1^2(t) \\ &+ \frac{1}{2} Y_2 u_2^2(t) + \lambda_1 S_h^* + \lambda_2 E_c^* + \lambda_3 E_m^* + \lambda_4 E_{mc}^* + \lambda_5 I_c^* + \lambda_6 I_m^* \\ &+ \lambda_7 I_{mc}^* + \lambda_8 I_{cEm}^* + \lambda_9 I_{mEc}^* + \lambda_{10} R_h^* + \lambda_{11} S_{\mathrm{v}}^* + \lambda_{12} E_{\mathrm{v}}^* + \lambda_3 I_{\mathrm{v}}^* \end{aligned} \tag{28}$$

The transversality conditions $\lambda_j(t_f) = 0, \qquad j = 1, 2, 3, \ldots, 13$ are satisfied. From Eq. (21), we obtain

$$\begin{aligned} \frac{\partial H}{\partial u_1} =& Y_1 u_1^* - \beta_m S_h(\lambda_3 - \lambda_1) - \beta_m E_c(\lambda_4 - \lambda_2) - \lambda_1 \beta_m I_c(\lambda_8 - \lambda_5) \\ &- \beta_{\mathrm{v}} S_{\mathrm{v}}(\lambda_{12} - \lambda_{11}) \\ \frac{\partial H}{\partial u_2} =& Y_2 u_2^* - \beta_c S_h(\lambda_2 - \lambda_1) + \beta_c E_m(\lambda_4 - \lambda_3) + \lambda_2 \beta_c I_m(\lambda_8 - \lambda_6) \end{aligned} \tag{29}$$

Therefore

$$\begin{aligned} u_1^* &= \max\left\{0, \min\left\{1, \frac{\mathfrak{B}_1}{Y_1}\right\}\right\} \\ u_2^* &= \max\left\{0, \min\left\{1, \frac{\mathfrak{B}_2}{Y_2}\right\}\right\} \end{aligned} \tag{30}$$

where $\mathfrak{B}_1 = \beta_m S_h(\lambda_3 - \lambda_1) + \beta_m E_c(\lambda_4 - \lambda_2) + \lambda_1 \beta_m I_c(\lambda_8 - \lambda_5) + \beta_{\mathrm{v}} S_{\mathrm{v}}(\lambda_{12} - \lambda_{11})$ and $\mathfrak{B}_2 = \beta_c S_h(\lambda_2 - \lambda_1) + \beta_c E_m(\lambda_4 - \lambda_3) + \lambda_2 \beta_c I_m(\lambda_8 - \lambda_6)$ □

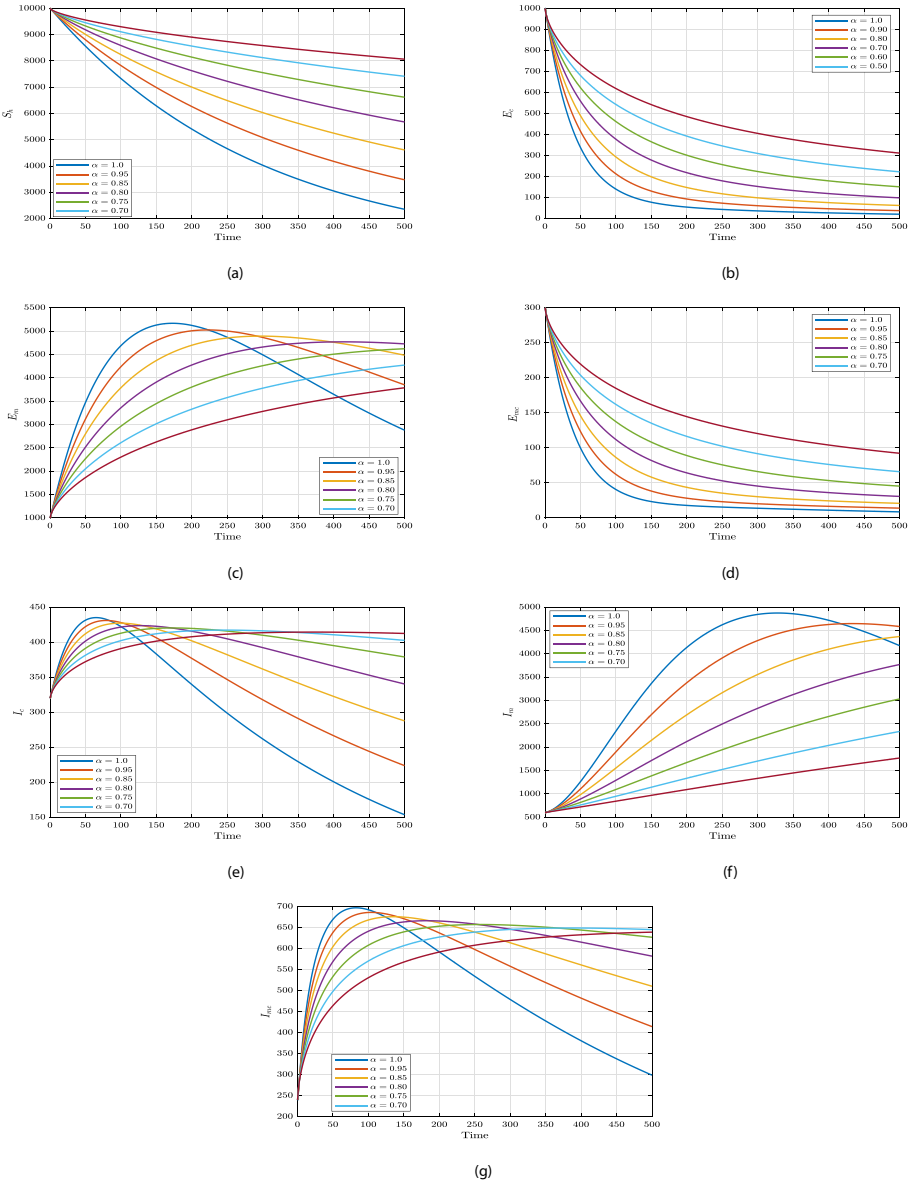

Fig. 2 Numerical trajectory of Covid-19-Malaria co-infection transmission under ABC fractional operator

This shows that the uniqueness of the fractional optimal control of the model has been established for small t_f due to prior boundedness of both state and adjoint variables. This is achieved by using Lipschitz property of the ordinary differential equations.

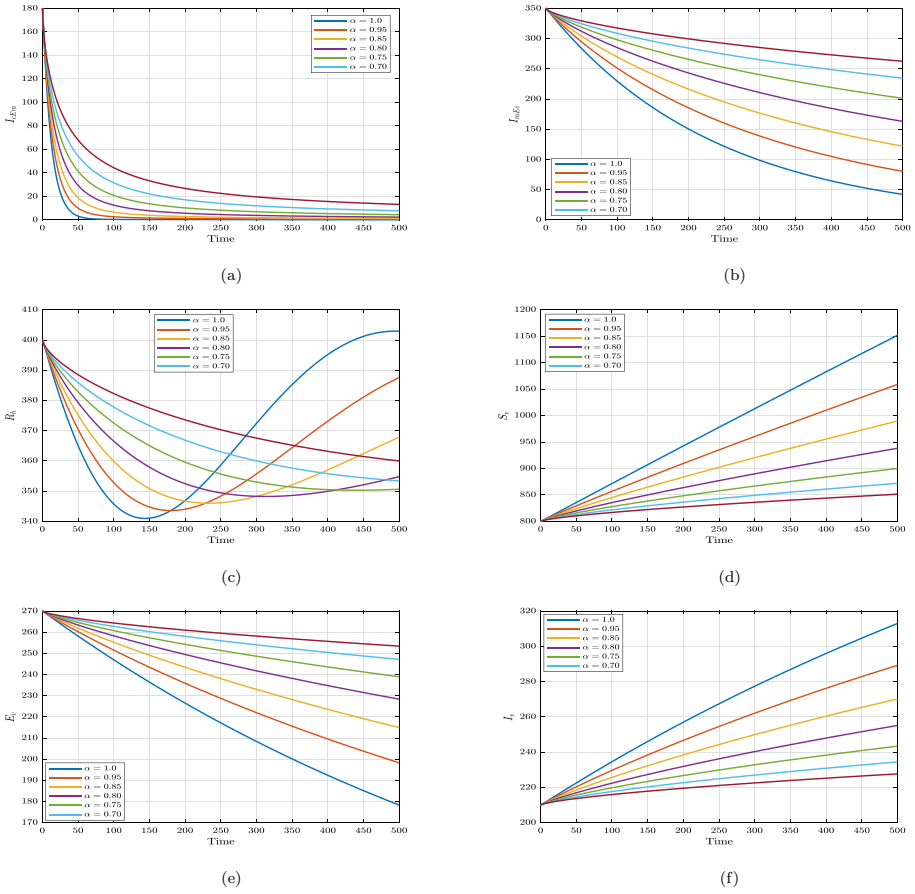

Fig. 3 Numerical trajectory of Covid-19-Malaria co-infection transmission under ABC fractional operator

5 Numerical results and discussion for Malaria and Covid-19 co-infection transmission model

This section of the study presents the fractional-order models numerical techniques to understand the behavior of the solution trajectories better. We compute the model associated with the ABC-fractional operator $\alpha \in (0.1)$ using the fractional Adams-Bashforth technique to gain insight into the solution trajectories. For this, use the following initial conditions: $S_h = 10000; E_c = 1000; E_m = 1000; E_{mc} = 300; I_m = 320; I_c = 600; I_{mc} = 240; I_{mEc} = 180;$ $I_{cEm} = 350; R_h = 400; S_v = 800; E_v = 270; I_v = 210$. We compare the effects of various fractional order values with of a step size 0.2 throughout the time range [0,500] against the parameter values listed in Table 1 on both human and non-human populations. Interestingly, the behaviour of both population is affected by changing the order of the fractional derivative, we observed distinct memory effects in each, as shown in Figs. 2 and 3. We observed an increase in the number of susceptible individuals, that is Fig. 2a as the number of recovered individuals Fig. 3c increased over time. This dynamics can be attributed to the direct relationship between infectious and recovered individuals. Similarly, in Fig. 2c–g

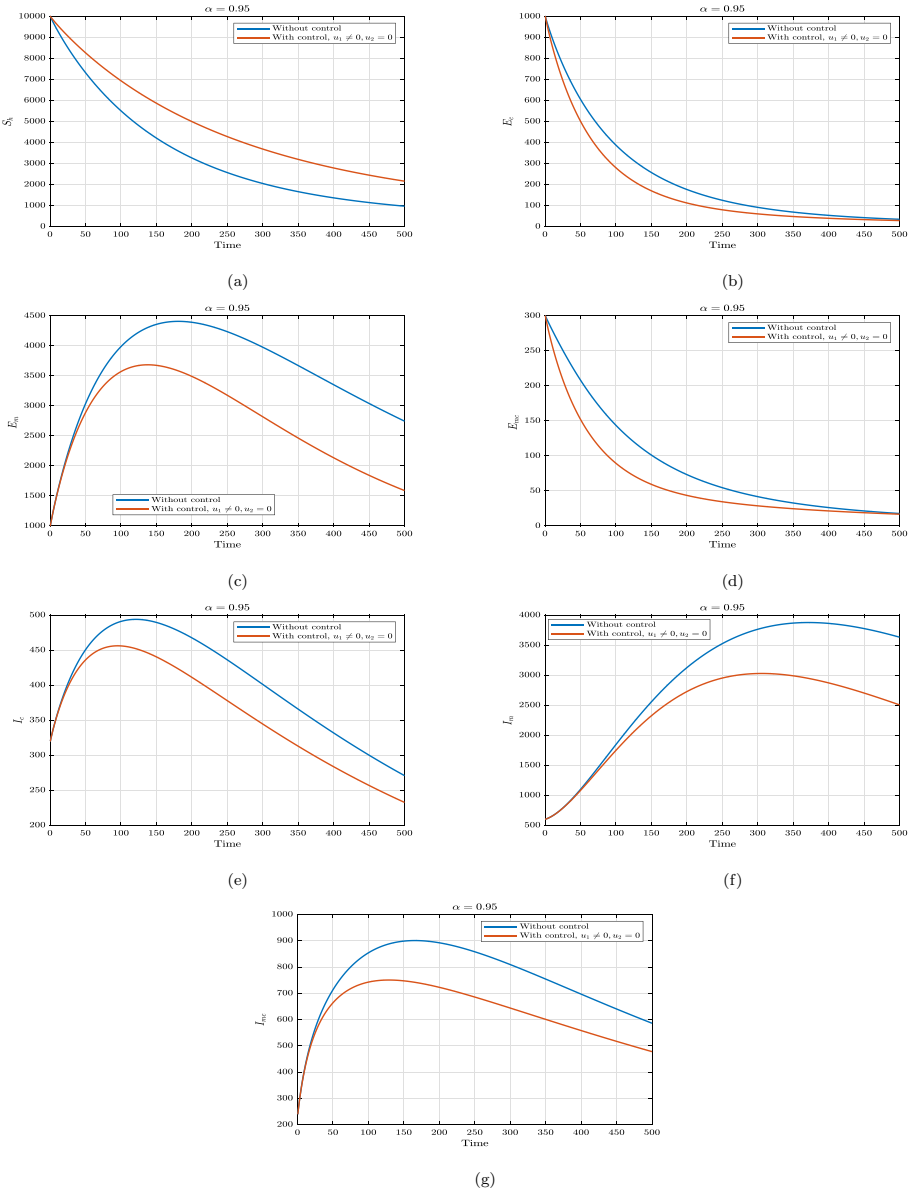

Fig. 4 Effects of varying values of u_1 on the dynamics of the Covid-19-Malaria co-infection at $\alpha = 0.95$

exhibit direct relationship between exposed and infectious individuals to malaria, Covid-19, and co-dynamics respectively. In biological perspective, these trajectories shows that whenever the population is highly expose to the virus or disease, the probability of getting infected is possibly high and vice versa. These graphs in Fig. 3d–f demonstrate how dependence the system is on the history of the mosquitoes and how sensitive it is to vary the fractional order α. Next, we investigate the impact of control strategies on the

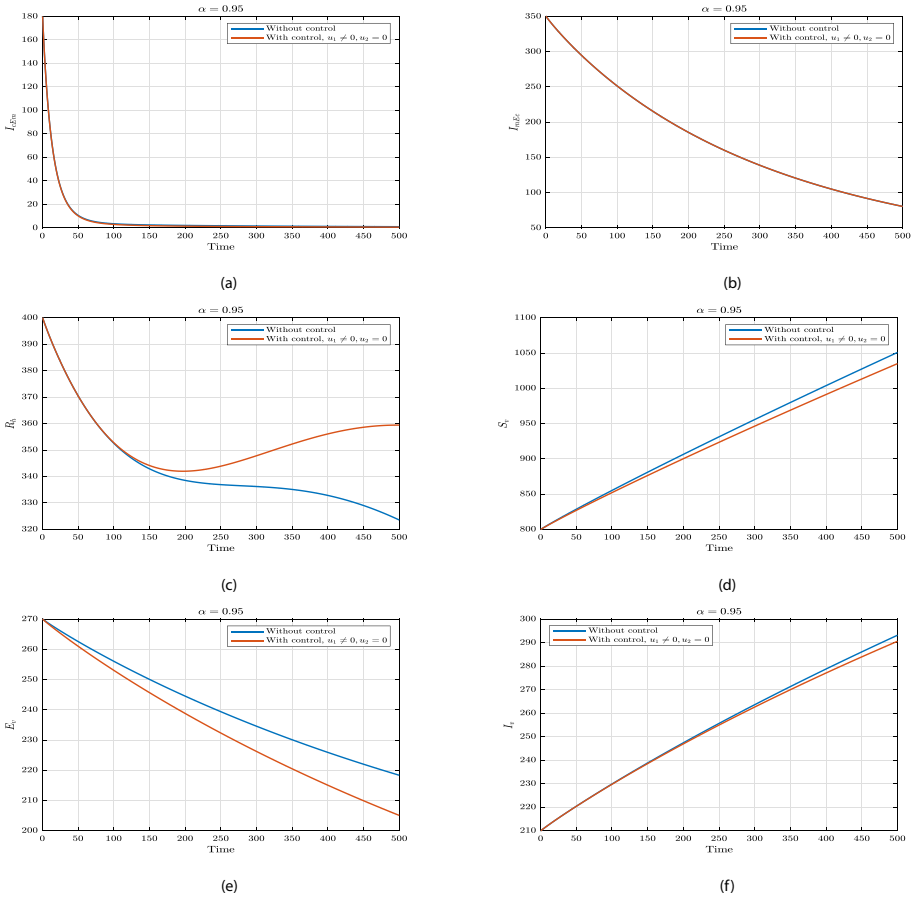

Fig. 5 Effects of varying values of u_1 on the dynamics of the Covid-19-Malaria co-infection at $\alpha = 0.95$

transmission dynamics of our proposed model in both human and mosquitoes population. The applied control interventions are described as follows:

1. Apply the use of personal protection measures to prevent mosquitoes bites during the day and the night such as the use of insecticide-treated nets, application of repellents to skin or spraying of insecticides at a time, that is $u_1(t)$.
2. Apply the use of personal protection measures to protect oneself again corona virus such as facial mask, hydro-alcoholic gel hand-washing with soap at a time, that is $u_2(t)$.
3. Apply combination of personal protection measures to prevent or protect oneself again corona virus and mosquitoes bites at a time, that is $u_1(t)$ and $u_2(t)$.

From strategy 1, which are Figs. 4 and 5 are used to optimize Malaria- Covid-19 co-infection transmission dynamics while neglecting the personal protection measures to protect oneself again corona virus at a time, $u_2(t)$. We observed a decrease in the number of

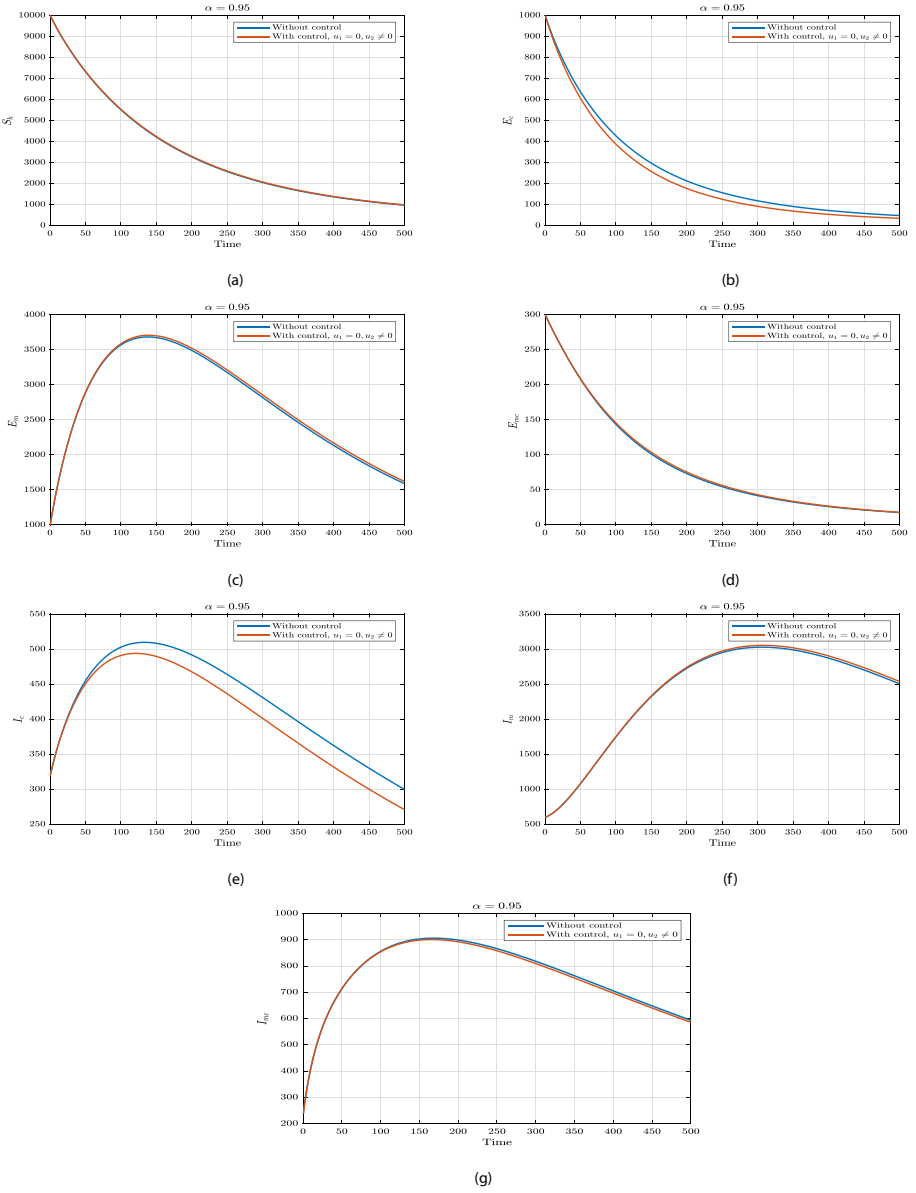

Fig. 6 Effects of varying values of u_2 on the dynamics of the Covid-19-Malaria co-infection at $\alpha = 0.95$

exposed and infection in both population and interestingly, a minimal decrease in co-infection transmission as presented in Fig. 5a and b.

Similarly, from strategy 2, which are Figs. 6 and 7 are used to optimize Malaria- Covid-19 co-infection transmission dynamics while neglecting the personal protection measures to prevent mosquitoes bites during the day and the night, $u_1(t)$. We observed a asymptotical

Table 1 Details definition of variables and parameters

Parameter	Value	Source	Parameter	Value	Source
Λ_h	$\frac{10000}{(59 \times 365)}$	Tchoumi et al. (2021)	α_c	0.4531	Tchoumi et al. (2021)
Λ_v	$\frac{10000}{21}$	Tchoumi et al. (2021)	α_{v}	0.48	Tchoumi et al. (2021)
ϕ_1	0.0833	Tchoumi et al. (2021)	ϕ_2	0.4	Tchoumi et al. (2021)
σ_m	0.8333	Tchoumi et al. (2021)	b	$4.3 * 0.33$	Tchoumi et al. (2021)
σ_c	0.6	Tchoumi et al. (2021)	δ_c	0.00286	Tchoumi et al. (2021)
σ_{v}	0.1	Tchoumi et al. (2021)	δ_m	0.068	Tchoumi et al. (2021)
σ_{mc}	0.333	Tchoumi et al. (2021)	$\delta_m c$	0.0383	Tchoumi et al. (2021)
λ_c	0.3	Tchoumi et al. (2021)	μ	$\frac{1}{(59 \times 365)}$	Tchoumi et al. (2021)
λ_m	0.25	Tchoumi et al. (2021)	η	$\frac{1}{21}$	Tchoumi et al. (2021)
υ	0.025	Tchoumi et al. (2021)	γ_1	$[0-1]$	Tchoumi et al. (2021)
ϵ	0.5	Tchoumi et al. (2021)	ϑ	0.5	Tchoumi et al. (2021)
α_m	0.125	Tchoumi et al. (2021)	γ_2	$[0-1]$	Tchoumi et al. (2021)
α_r	0.5	assumed			

decrease in the number of exposed and infection in human population and a very minimal co-infection transmission. From Fig. 7d,e,f, which are mosquitoes population, we observed no significant impact and this dynamics means that personal protection measures to protect oneself again corona virus at a time, $u_2(t)$ has nothing to do with mosquitoes population.

Finally, from strategy 3, which are Figures of 8 and 9 are used to optimize Malaria-Covid-19 co-infection transmission dynamics. We applied combination of personal protection measures to prevent or protect oneself again corona virus and mosquitoes bites at a time, that are $u_1(t)$ and $u_2(t)$. We observed a significant decrease in the number of exposed and infection in both population and interestingly, a high decrease in co-infection transmission.

6 Conclusion

The impact of control strategies on malaria and COVID-19 coinfection through our fractional order mathematical model yields promising results, providing critical insights into the effectiveness of various intervention measures. The model incorporates three key control strategies:$u_1(t)$ represents the use of personal protection measures to prevent mosquitoes bites during the day and the night such as the use of insecticide-treated nets, application of repellents to skin or spraying of insecticides at a time t, $u_2(t)$ represents practising physical distancing, maintaining good hand hygiene, and avoiding large gatherings. Our numerical simulations demonstrate that the implementation of personal protection measures targeting malaria, such as insecticide-treated nets, repellents, and indoor residual spraying, significantly reduces the transmission rates of malaria-causing

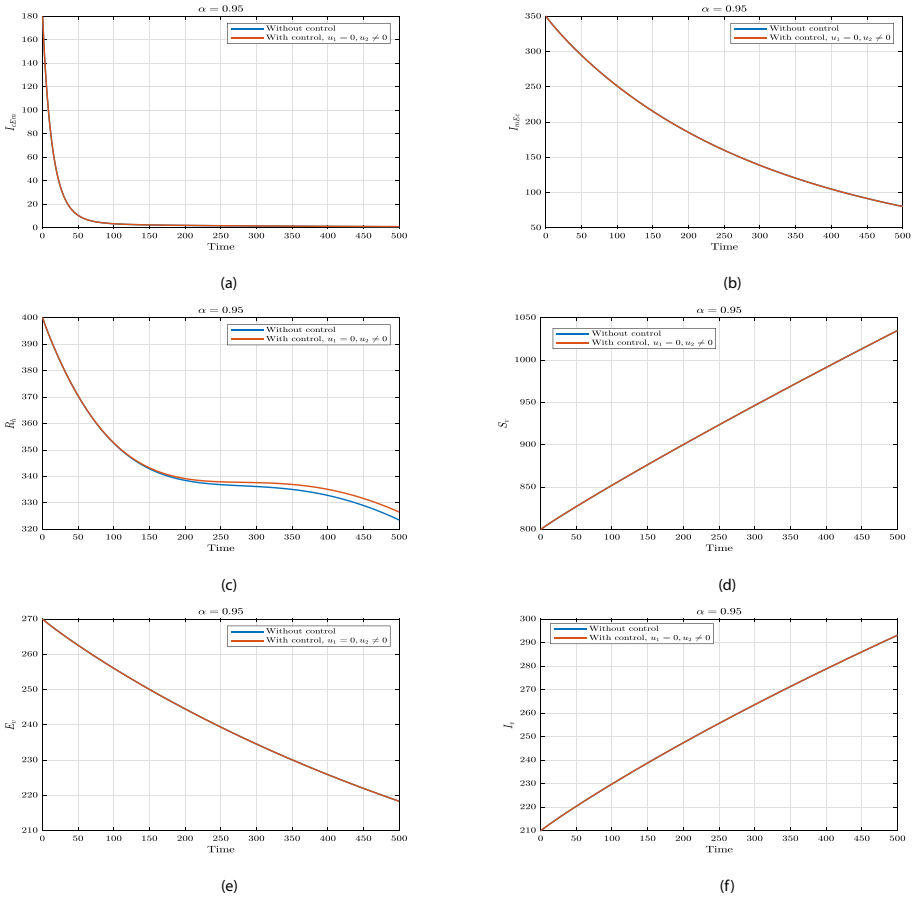

Fig. 7 Effects of varying values of u_2 on the dynamics of the Covid-19-Malaria co-infection at $\alpha = 0.95$

parasites. Additionally, the adoption of personal protection measures against COVID-19, including the use of facial masks, hand hygiene with hydro-alcoholic gel or soap, proves effective in controlling the spread of the coronavirus.

However, the most substantial impact on mitigating the burden of coinfection is observed when individuals consistently apply a combination of personal protection measures ($u_1(t)$ and $u_2(t)$) to prevent both malaria and COVID-19. This integrated approach demonstrates synergistic effects, leading to a more significant reduction in the overall disease transmission rates.

Our findings underscore the importance of individual behaviors and public health efforts in controlling the spread of both diseases. Adherence to personal protection measures, irrespective of the targeted pathogen, plays a crucial role in limiting transmission

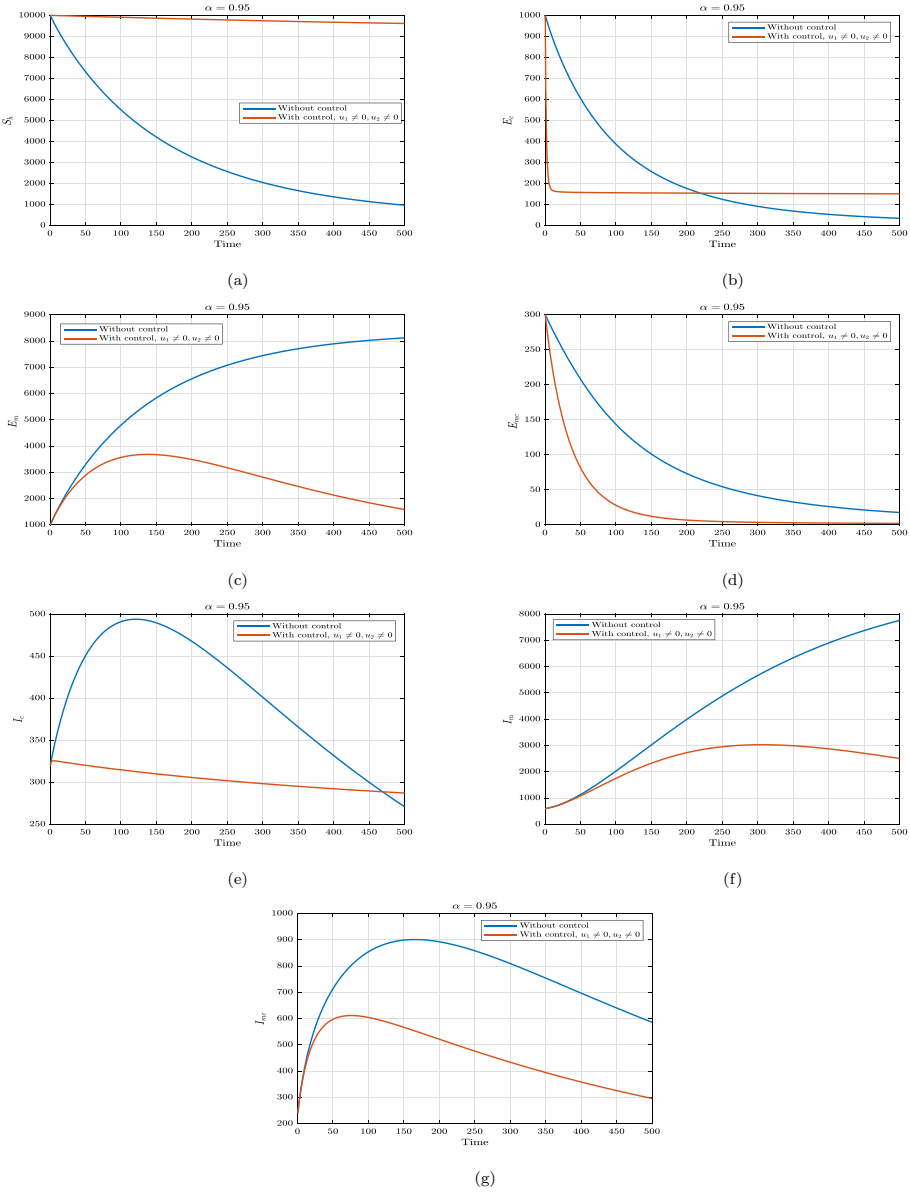

Fig. 8 Effects of varying values of $u_1 = u_2$ on the dynamics of the Covid-19-Malaria co-infection at $\alpha = 0.95$

and protecting vulnerable populations. Furthermore, the results emphasize the value of comprehensive public health interventions that address both malaria and COVID-19 simultaneously.

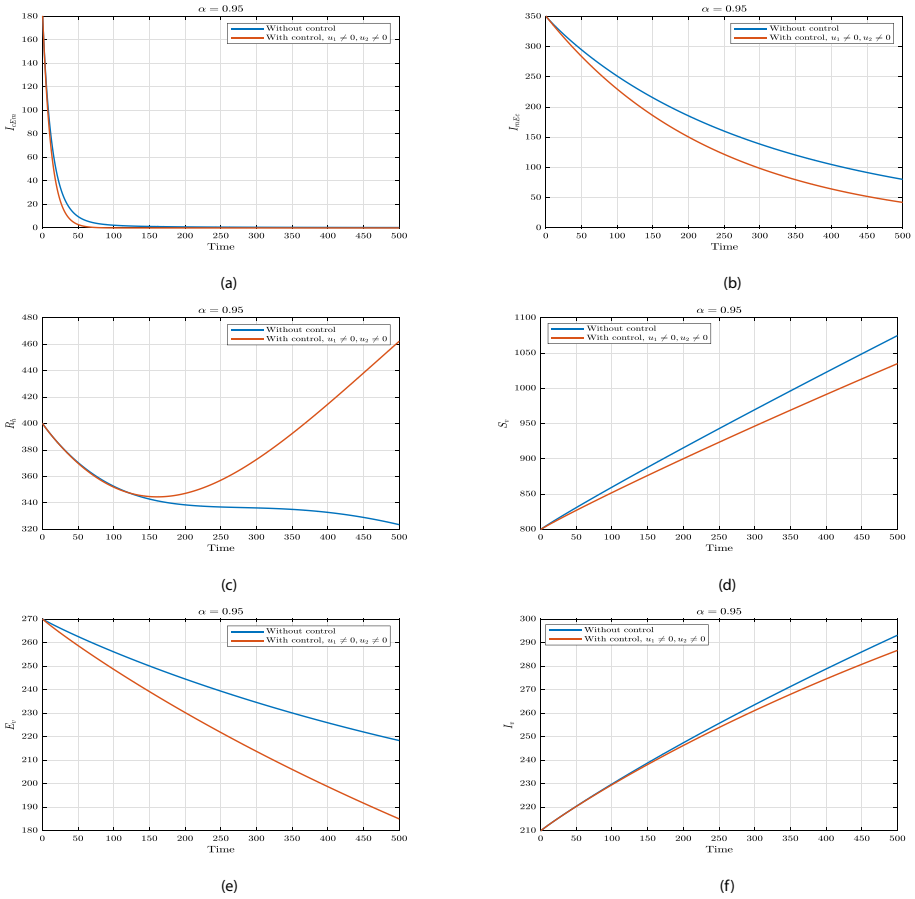

Fig. 9 Effects of varying values of $u_1 = u_2$ on the dynamics of the Covid-19-Malaria co-infection at $\alpha = 0.95$

The application of a fractional order mathematical model in this study provides a more nuanced understanding of the coinfection dynamics. The incorporation of non-integer derivatives allows for a more accurate representation of complex interactions and system behaviors, enhancing the model's predictive capacity.

In conclusion, the insights gained from our study contribute to the development of targeted and efficient control strategies for the dual burden of malaria and COVID-19. By promoting the consistent use of personal protection measures and integrated health interventions, public health authorities can make substantial progress in reducing the transmission and impact of both diseases. These findings highlight the significance of a multidisciplinary approach in combating the coinfection of malaria and COVID-19, ultimately improving global health outcomes and saving lives.

Data availability Data used to support the findings of this study are included in the article. The authors used a set of parameter values whose sources are from the literature as shown in Table 1.

Declarations

Competing interest The authors declare that they have no known competing financial interests or personal relationships that could have appeared to influence the work reported in this paper.

Human and animal rights This article does not contain any studies with human or animal subjects.

References

Abioye, A.I., Ibrahim, M.O., Peter, O.J., Ogunseye, H.A.: Optimal control on a mathematical model of malaria, Sci. Bull. A. Appl0 Math. Phy. 178–190 (2020)

Abioye, A.I., Peter, O.J., Ogunseye, H.A., Oguntolu, F.A., Ayoola, T.A., Oladapo, A.O.: A fractional-order mathematical model for malaria and Covid-19 co-infection dynamics. Healthcare Anal. 100210 (2023)

Abioye, A.I., Ibrahim, M.O., Peter, O.J., Amadiegwu, S., Oguntolu, F.A.: Differential transform method for solving mathematical model of SEIR and SEI spread of malaria. Int. J. Sci. Basic Appl. Res. (IJSBAR) **40**(1), 197–219 (2018)

Addai, E., Adeniji, A., Peter, O.J., Agbaje, J.O., Oshinubi, K.: Dynamics of age-structure smoking models with government intervention coverage under fractal-fractional order derivatives. Fractal Fraction. **7**(5), 370 (2023)

Atangana, A., Baleanu, D.: New fractional derivatives with nonlocal and non-singular kernel: theory and application to heat transfer model. arXiv preprint arXiv:1602.03408 (2016)

Avusuglo, W., Han, Q., Woldegerima, W.A., Bragazzi, N.L., Ahmadi, A., Asgary, A., Wu, J., Orbinski, J., Kong, J.D.: Covid-19 and malaria co-infection: do stigmatization and self-medication matter? A mathematical modelling study for nigeria, A mathematical modelling study for Nigeria (2022)

Boltyanskiy, V., Gamkrelidze, R.V., Mishchenko, Y., Pontryagin, L.: Mathematical theory of optimal processes. Wiley (1962)

Bwire, G.M., Paulo, L., Mduma, E.: Coinfection of malaria and COVID-19: a systematic review. J. Trop. Med. **2020**, 6386396 (2020). https://doi.org/10.1155/2020/6386396

Chanda-Kapata, P., Kapata, N., Zumla, A.: Modeling the dual burden of malaria and COVID-19 in Sub-Saharan Africa. J. Travel Med. **27**, taaa121 (2020). https://doi.org/10.1093/jtm/taaa121

Maayah, B., Moussaoui, A., Bushnaq, S., Abu Arqub, O.: The multistep Laplace optimized decomposition method for solving fractional-order coronavirus disease model (COVID-19) via the caputo fractional approach. Demonstratio Math. **55**(1), 963–977 (2022)

Maayah, B., Arqub, O.A., Alnabulsi, S., Alsulami, H.: Numerical solutions and geometric attractors of a fractional model of the cancer-immune based on the Atangana–Baleanu–Caputo derivative and the reproducing kernel scheme. Chin. J. Phys. **80**, 463–483 (2022)

Mekonen, K.G., Balcha, S.F., Obsu, L.L., Hassen, A.: Mathematical modeling and analysis of TB and COVID-19 coinfection. J. Appl. Math. **2022**, 1–20 (2022)

Momani, S., Abu Arqub, O., Maayah, B.: Piecewise optimal fractional reproducing kernel solution and convergence analysis for the Atangana–Baleanu–Caputo model of the Lienard's equation. Fractals **28**(08), 2040007 (2020)

Momani, S., Maayah, B., Arqub, O.A.: The reproducing kernel algorithm for numerical solution of van der pol damping model in view of the Atangana–Baleanu fractional approach. Fractals **28**(08), 2040010 (2020)

Ojo, M.M., Goufo, E.F.D.: The impact of COVID-19 on a malaria dominated region: a mathematical analysis and simulations. Alex. Eng. J. **65**, 23–39 (2023)

Ojo, M.M., Benson, T.O., Peter, O.J., Goufo, E.F.D.: Nonlinear optimal control strategies for a mathematical model of COVID-19 and influenza co-infection. Physica A **607**, 128173 (2022)

Okuonghae, D., Omame, A.: Analysis of a mathematical model for COVID-19 population dynamics in Lagos, Nigeria. Chaos Solitons Fractals **139**, 110032 (2020)

Omame, A., Rwezaura, H., Diagne, M., Inyama, S., Tchuenche, J.: COVID-19 and dengue co-infection in brazil: optimal control and cost-effectiveness analysis. European Phys. J. Plus **136**(10), 1090 (2021)

Orwa, T.O., Mbogo, R.W., Luboobi, L.S.: Optimal control analysis of hepatocytic-erythrocytic dynamics of plasmodium falciparum malaria. Infect. Dis. Modell. **7**(1), 82–108 (2022)

Peter, O.J., Shaikh, A.S., Ibrahim, M.O., Nisar, K.S., Baleanu, D., Khan, I., Abioye, A.I.: Analysis and dynamics of fractional order mathematical model of Covid-19 in Nigeria using Atangana–Baleanu operator (2021)
Peter, O.J., Shaikh, A.S., Ibrahim, M.O., Nisar, K.S., Baleanu, D., Khan, I., Abioye, A.I.: Analysis and dynamics of fractional order mathematical model of COVID-19 in Nigeria using Atangana–Baleanu operator. Comput. Mater. Continua **66**(2), 1823–1848 (2021)
Peter, O.J., Yusuf, A., Ojo, M.M., Kumar, S., Kumari, N., Oguntolu, F.A.: A mathematical model analysis of meningitis with treatment and vaccination in fractional derivatives. Int. J. Appl. Comput. Math. **8**(3), 117 (2022)
Peter, O.J., Oguntolu, F.A., Ojo, M.M., Olayinka Oyeniyi, A., Jan, R., Khan, I.: Fractional order mathematical model of monkeypox transmission dynamics. Phys. Scr. **97**(8), 084005 (2022)
Sweilam, N., AL-Mekhlafi, S., Albalawi, A.: Optimal control for a fractional order malaria transmission dynamics mathematical model. Alex. Eng. J. **59**(3), 1677–1692 (2020)
Tchoumi, S., Diagne, M., Rwezaura, H., Tchuenche, J.: Malaria and COVID-19 co-dynamics: a mathematical model and optimal control. Appl. Math. Model. **99**, 294–327 (2021)
Tchoumi, S., Diagne, M., Rwezaura, H., Tchuenche, J.: Malaria and COVID-19 co-dynamics: a mathematical model and optimal control. Appl. Math. Model. **99**, 294–327 (2021)
Wang, Y., Chen, Y., Li, Y., Yang, Y.: Epidemiological dynamics of COVID-19 and malaria co-infection: an up-to-date review. Front. Med. **7**, 595843 (2020). https://doi.org/10.3389/fmed.2020.595843
Wesolowski, A., Eagle, N., Tatem, A.J., Smith, D.L., Noor, A.M., Snow, R.W., Buckee, C.O.: Quantifying the impact of COVID-19 control measures on malaria transmission. Nat. Commun. **11**, 5710 (2020). https://doi.org/10.1038/s41467-020-19442-1
Zhu, C., Liang, L., Peng, G., Yuan, H., Zhou, L., Li, Y., Zhang, L., Lu, L.: Explosion plume on the exit surface of fused silica during UV laser-induced damage. Res. Phys. **32**, 105094 (2022)